

Строительные материалы и изделия
Construction Materials and Products

journal homepage: https://bstu-journals.ru

ISSN
2618-7183

DOI: 10.58224/2618-7183-2026-9-5-2

A field comparison of the thermal performance of ventilated and plastered façades in hot conditions using the climate of Southern Kazakhstan as an example: internal surface temperature and air conditioning energy efficiency

Zhangabay N.Zh. [1], Suleimenov U.S. [1], Utelbayeva A.B. * [1], Aidarova A.B. [1], Kolesnikov A.S. [1], Tursunkulov I.B. [1], Tursunkululy T. [1], Nazmi M.N. [2]

[1] M. Auezov South Kazakhstan University, Kazakhstan,
[2] Universiti Putra Malaysia (UPM), Malaysia

Abstract. This paper presents a field (full-scale) study comparing the thermal performance of a ventilated rainscreen façade (VRF) and a traditional plastered ("wet") façade on the eastern façade of a nine-story reinforced concrete frame residential building in Southern Kazakhstan during a hot summer period. Sensor-equipped sections of the multilayer wall structure from the 1st to the 9th floors were monitored simultaneously using DS18B20 multichannel contact temperature sensors, an unmanned thermal imaging system (DJI Mavic 3 Thermal), and a handheld thermal imager (Testo 875), providing double, independent validation of surface temperature data. Measurements were taken at 9:00, 12:00, 15:00, and 18:00 on a typical hot day. Although the temperature of the VRF exterior cladding during peak insolation hours exceeded the temperature of the wet façade by up to 2.2°C (reaching 60.1°C on the ninth floor at midday), the temperature of the VRF internal surface was consistently lower than the temperature of the wet façade internal surface on virtually all floors and at all times, the decrease reached 1.55°C, and averaged 1.0-1.3°C during the hottest hours. This apparent paradox, a hotter exterior cladding with a cooler internal surface, is explained by convective decoupling, which is provided by the ventilated air gap: it removes solar-heated air before it has a chance to transfer heat to the load-bearing wall via conduction. Based on the measured temperature difference of the internal surface and its standard heat transfer coefficient, it was shown that the conductive-convective component of the air-conditioning load for rooms behind the VRF is reduced by approximately 7-10% compared to a wet façade during typical hot daytime hours. These results, which relate to the relatively little-studied hot arid/continental climate of Central Asia, expand the evidence base, formed primarily from Mediterranean and Western European studies, and create a natural experimental basis for further thermal and aerodynamic modeling of the ventilated air gap.

Keywords: ventilated rainscreen façade, plastered ("wet") façade, hot climate, internal surface temperature, infrared thermography, energy efficiency of cooling systems, life safety, Central Asia, walling

*Corresponding author E-mail: mako_01-777@mail.ru

Received May 12, 2026; Received in revised form July 9, 2026; Accepted September 6, 2026

Please cite this article as: Zhangabay N.Zh., Suleimenov U.S., Utelbayeva A.B., Aidarova A.B., Kolesnikov A.S., Tursunkulov I.B., Tursunkululy T., Nazmi M.N. A field comparison of the thermal performance of ventilated and plastered façades in hot conditions using the climate of Southern Kazakhstan as an example: internal surface temperature and air conditioning energy efficiency. Construction Materials and Products. 2026. 9 (5). 2. DOI: 10.58224/2618-7183-2026-9-5-2

1. INTRODUCTION

Buildings account for approximately 30% of global final power delivery [1], with the share related to air conditioning being the fastest growing component of this demand: according to the International Energy Agency, it will grow by almost 4% per year until 2035 as incomes, population size and average temperatures increase [2, 3]. Since opaque (blind) walls typically comprise the largest area of a building's walling, their ability to attenuate solar and external heat gains before they reach the interior is a key lever for reducing the operational load on air conditioning, especially in hot arid and hot continental climates, where wall surface temperatures under direct solar irradiation can exceed 55-60 °C [2, 3]. Ventilated rainscreen façades (VRF) are structures in which the external cladding is separated from the load-bearing wall and frost protection by an open, naturally ventilated air gap, are widely promoted as a passive means of reducing this heat flow, and their use in renovation and new construction has been steadily increasing over the past two decades [4, 5].

The physical mechanism by which a VRF should outperform a directly plastered ("wet") façade is the convective removal of solar-heated air from the interlayer by gravitational convection and wind, which "decouples" the inward-facing wall from the peak equivalent (sol-air) temperature acquired by the cladding under direct solar irradiation [4, 6]. Early analytical and CFD studies quantitatively substantiated this mechanism: Balocco [6] proposed one of the first simplified steady-state heat balance models for a ventilated facade; Ciampi, Leccese and Tuoni [7] showed, using a mathematical model of a number of opaque VRF configurations, that the reduction in summer cooling load depends significantly on the interlayer thickness, the position of the insulation and the absorptivity of the cladding; using a double-layer façade as an example, Gratia and De Herde [8] demonstrated that natural ventilation strategies significantly reduced cooling energy delivery compared to a sealed interlayer. However, these seminal studies relied primarily on numerical or laboratory models of reduced scale rather than on in-kind monitoring of multi-story buildings under real operating conditions, leaving open the question of how the predicted interlayer behavior manifests itself in real buildings under actual wind, solar, and operating conditions.

Subsequent experimental campaigns have partially closed this gap for specific climate conditions. Sanjuan et al. [9] compared a ventilated façade with open joints and a traditional façade with a sealed interlayer and recorded summer energy savings of about 26% under high insolation; Marinosci et al. [10] performed an empirical validation of a naturally ventilated screen façade on a full-scale building; Stazi et al. [11] evaluated ventilated walls with clay cladding; Labat et al. [12] and Tong and Li [15] investigated open joint cladding and sloped ventilated roofs under direct solar irradiation, respectively. Gagliano et al. [13] extended these findings to ventilated roofs. Taken together, these studies confirm the cooling benefits of ventilation in Mediterranean and temperate Atlantic climates, but virtually none of them provide the temperature of the interior (room-facing) surface at several elevations of an operational multi-story building, measured simultaneously with the temperature of an adjacent non-ventilated reference area of the same façade; it is precisely this comparison that is the focus of this study.

More recent works have begun to cover colder and mixed climate zones and more complex VRF configurations. Yu, Yang, and Xiong [14] studied the dynamic thermal performance of ventilated hollow-core walls; Zhao et al. [16] numerically investigated an VRF equipped with a heat recovery unit and a latent heat accumulator; Gagliano and Aneli [17] analyzed the performance of an opaque VRF in both winter and summer conditions; Karanafti, Theodosiou, and Tsikaloudaki [18] provided a review of dynamic thermal insulation technologies, which was later developed by Karanafti and Theodosiou [20] for VRF operating on the dynamic thermal insulation principle; Lin, Song, and Chu

[19] conducted full-scale summer/winter tests of an opaque VRF in a cold climate zone of China; Wang, Chen, and Zhou [29] modeled a ventilated double-layer façade for a hot-summer, cold-winter zone of China; and Domínguez-Torres et al. [21], Roig et al. [22], and De Masi et al. [23] have performed parametric optimization of VRF configurations (wall types, cladding, recycled insulation) for a Mediterranean climate in the past two years. Two comprehensive reviews, Ibañez-Puy et al. [4] and, more recently, Pizzatto et al. [5], systematize this body of work and both explicitly note that the geographic distribution of experimental VRF studies is heavily skewed toward Mediterranean Europe, continental China, and, to a lesser extent, the tropical/arid climates of the Persian Gulf countries, while the hot arid continental climates of Central Asia are largely absent from the evidence base reviewed. None of these reviews, nor any of the listed primary works, provide a comparison of the VRF and an unprocessed reference "wet" façade on the same building, with a floor-by-floor resolution, validated by two independent thermal imaging methods, it is precisely this methodological configuration that is adopted in this work.

Since the ventilated interlayer is both a structural and aerodynamic element, a number of studies have focused on its mechanical behavior and airflow patterns, rather than solely on its thermal characteristics. Pankratov [24] proposed a nonlinear analytical model for temperature distribution in the ventilated interlayer; Di Nunzio et al. [25] investigated the in-plane behavior of lightweight façade systems under seismic loading, which is relevant for VRF assemblies in seismically active regions, including Southern Kazakhstan. These studies emphasize that the interlayer width, fastening geometry, and airflow path, parameters that vary from project to project and are rarely provided along with thermal results, significantly affect both the structural and thermal performance of the VRF, reinforcing the need to obtain in-kind data for a specific project rather than transferring generalized coefficients from other climatic conditions or geometries.

From a diagnostic perspective, infrared thermography (IR thermography) has become a standard non-destructive method for assessing the condition of building envelopes, and the associated measurement and calculation uncertainty assessment procedures are codified in international standards such as ISO 6946 [30] and ISO 10211:2017 «Thermal Bridges in Building Construction – Heat Flows and Surface Temperatures – Detailed Calculations». However, most published in-situ VRF studies rely on only one measurement method (either embedded sensors or ground-based IR thermography), making surface temperature results vulnerable to local anomalies, emissivity errors, or sensor drift. This study addresses this issue by cross-validating multichannel contact sensor readings with two independent IR thermography methods, an unmanned aerial shooting (covering the entire nine-story façade) and a handheld thermal imager, at each measurement point and time.

A parallel body of literature has focused on how façade material and cladding choices affect external thermal conditions and the urban heat island, rather than directly affecting the indoor environment: Tabatabaei and Fayaz [26] quantified the impact of façade cladding on mitigating the urban heat island effect and outdoor comfort in a hot semi-arid climate; Hong et al. [27] reviewed cool façade strategies for reducing the urban heat island; and Maciel and Carvalho [28] developed a methodology for estimating the operational energy savings of opaque VRFs in Brazilian multi-story residential buildings. These studies confirm that façade-level interventions have measurable, climate-sensitive impacts on cooling demand, but, with the partial exception of the work of Maciel and Carvalho [28], they typically derive energy savings through building energy modeling rather than directly from measured internal surface temperature differences in the actual building, which is the approach used in Section 3.4 of this paper. General data from building physics on the optimization of wall thermal insulation and reduced heat transfer resistance [31], as well as the applicable national regulations SP RK 2.04-01-2017 «Construction Climatology» and SP RK 2.04-107-2013 «Thermal Performance of Buildings» form the normative-physical basis for the selection of the calculated internal temperature and measurement date used in the performance assessment in this work.

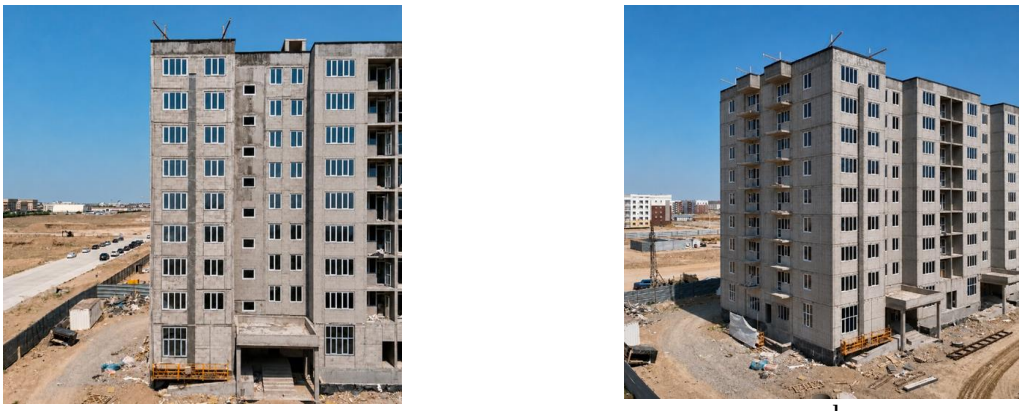
This study draws directly on the research program conducted by the authors' team on attached and adaptive façade systems in the climatic conditions of Southern Kazakhstan. Zhangabay et al. [32] reviewed the energy performance and operational loads of adaptive dynamic façades worldwide and concluded that the ventilated interlayer concept has been well studied analytically but has received little experimental support in hot continental climates; Rahiminejad and Khovalyg [33] experimentally characterised the hydrodynamic and thermal behaviour of the ventilated interlayer in attached façade

systems and showed that existing airflow models do not fully account for the combined effects of solar irradiation and vertical temperature gradients, which confirms the need for in-kind experimental studies. The most closely related to the present work is the accompanying full-scale study by Zhangabay et al. [34], which presents the diurnal and altitude dynamics of temperature fields on a building of the same height class (nine floors), as well as on an additional twenty-five-story building, under the influence of solar irradiation, and analyzes the thermal inertia and the influence of the interlayer geometry on heat transfer. This experimental line of work is methodologically consistent with the authors' broader research on the structural behavior and material characteristics of building envelopes and related infrastructure, including finite-difference modeling of the quasistatic motion of shallow concrete shells [35], an investigation of the mechanical characteristics and physical-and-chemical properties of slag-filled concretes using a metaheuristic predictive approach [36], and a review of the factors affecting extended avalanche destructions on long-distance gas pipelines [37], which together inform the materials- and structures-oriented perspective underlying the present study. This line of enquiry is consistent with recent work on the thermophysical behaviour of building materials and envelopes, in which the thermophysical characteristics of variatropic concretes and the resulting gain in heat-transfer resistance were quantified numerically [38], the heat and mass transfer accompanying the handling of concrete mixtures was described analytically [41], and cement composites intended specifically for dry and hot climates were designed and tested [40]; at the building scale, the same body of work addresses low-carbon life-cycle management of buildings [39] and the influence of the heat resistance of enclosing structures on the choice and placement of heating devices [42]. At the same time, in this study, the enclosing structure with the VRF was characterized in isolation: it did not directly compare the VRF with an adjacent, directly comparable reference section of the "wet" façade on the same façade of the same building, the ratio of the temperatures of the external and internal surfaces was not explicitly disclosed as a phenomenon of convective "decoupling", and the measured temperature difference of the internal surface was not translated into an assessment of the consequences for energy delivery for cooling. Addressing this gap, comparing VRF and wet façade on the same building, with floor-by-floor resolution, validated by two IR thermography methods, combined with an approximate assessment of cooling efficiency, is the specific objective of this paper.

Based on the above identified gaps, this work makes the following contributions: (i) a direct, floor-by-floor (1st, 5th, and 9th floors) and hourly (9:00-18:00) comparison of the external and internal surface temperatures of the VRF and the adjacent wet façade on the same building façade rather than in separate test cells or in simulated cases; (ii) a triangulated validation of the temperature field by three independent methods (embedded DS18B20 sensors, unmanned and handheld thermal imaging); (iii) an explicit disclosure and quantification of the counterintuitive relationship in which the external VRF surface is warmer than the wet façade while the internal surface is colder, explaining this phenomenon by convective "decoupling" in the ventilated interlayer; (iv) a rough, measurement-based estimate of the resulting reduction in the conductive component of the cooling load, expressed as a percentage rather than just as a temperature difference; and (v) climate-specific data for the hot, arid/continental climate of Southern Kazakhstan, a region that is largely unrepresented in the existing VRF literature discussed above. The practical significance of the study lies in the fact that designers and regulators in Central Asia receive in-kind, rather than transferable from other climatic conditions, VRF performance indicators for decision-making during renovation and new construction, while the scientific novelty lies in the combination of triple validation of in-kind measurements with a transparent, reproducible method for converting the measured surface temperature gain into an operational cooling energy efficiency indicator.

2. METHODS AND MATERIALS

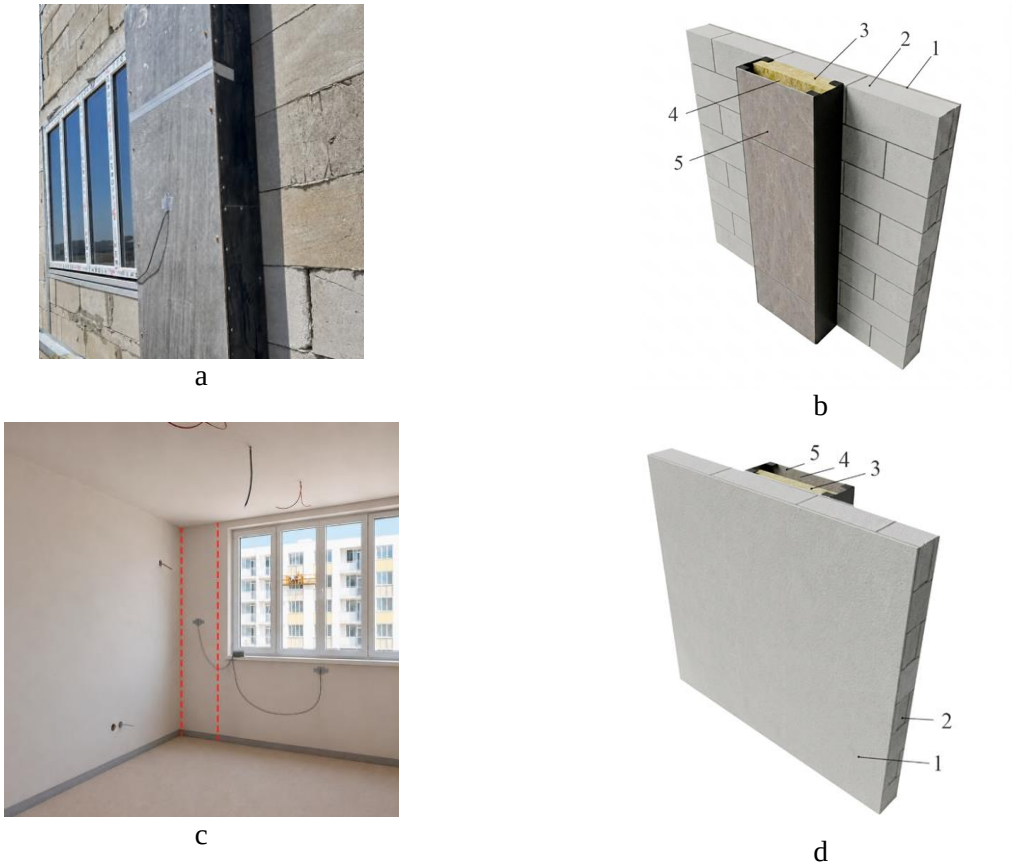
The study object was a multi-story (9-story) reinforced concrete frame residential building with a multi-layer wall structure. Each floor was 3 meters high. To ensure the reliability of the experimental data, the building was selected to exclude the influence of additional parameters, such as air conditioning or forced ventilation. The eastern façade of the building was examined (Fig. 1).



a b

Fig. 1. Object of study: (a) front view; (b) side view.

A rectangular structure 20 cm wide and 60 cm long with ceramic granite cladding was fabricated as a model of a ventilated rainscreen façade (VRF). To compare the effect of the VRF on interlayer temperature readings, the vertical structure was installed across the entire height of the building, spanning floors one through nine. This allowed to compare the internal surface temperatures of rooms in areas with the VRF model installed and in areas without a VRF (a traditional “wet” façade). The primary locations of the VRF and wet façade sections are shown in Fig. 2, and the design parameters are listed in Table 1.



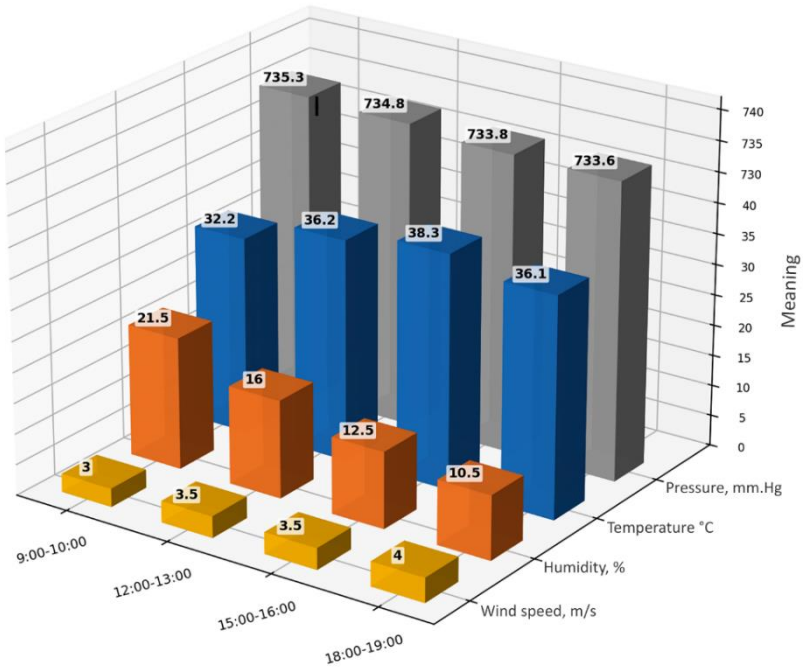
a b c d

Fig. 2. Rectangular structure of the VRF model: (a) photo of the external part of the wall; (b) model diagram, external side; (c) photo of the internal part of the wall; (d) model diagram, internal side.

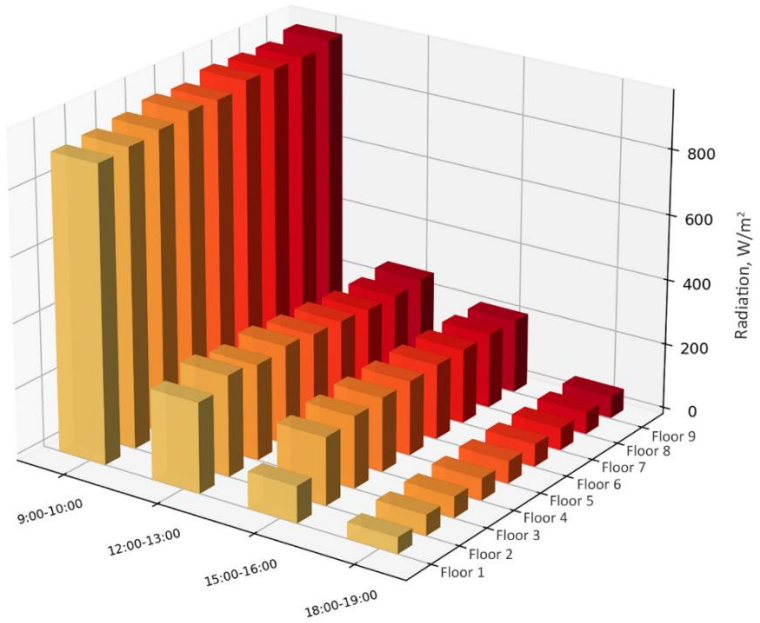
Table 1. Structural parameters of a multilayer walling.

Layer No. (according to Figure 2b)	Layer Name	Thickness, cm	Conduction, W/(m·°C)
1	Plastering	1.0	≈0.76
2	Gas Concrete Assembly	20.0	≈0.15
3	Thermal Insulation	10.0	≈0.036
4	Ventilated Air Gap	10.0	–
5	Ceramic Granite	1.0	≈3.5

Fig. 3 presents the climatic conditions of the study period. July 5th was chosen as the measurement date, a day corresponding to the hottest month according to the Republic of Kazakhstan Code of Practice on Construction Climatology SP RK 2.04-01-2017 «Construction Climatology». Hourly air temperature values were taken from meteorological data for the measurement period, and solar irradiation values were measured directly on-site using a pyranometer with an RS-485 interface.



a



b

Fig. 3. Climatic conditions during the measurement campaign: (a) air temperature, relative humidity, wind speed and atmospheric pressure at 9:00, 12:00, 15:00 and 18:00; (b) solar irradiation intensity by hour and by floor.

The temperatures of the external and internal surfaces of the multilayer external walling were measured using multichannel universal temperature sensors based on the DS18B20 chip with a measurement range of –55°C to +125°C. To ensure the reliability of the obtained interlayer temperature values, thermal imaging of the external and internal surfaces of the walling was additionally conducted using a DJI Mavic 3 Thermal quadcopter (thermal imaging resolution of 640 × 512 pixels) for the external surface and a Testo 875 handheld thermal imager (resolution of 160 × 120 pixels) for the internal surface.

The experimental methodology was built on the principle of reliability through double independent validation of the measured values, achieved by parallel, simultaneous recording of the temperature field using two physically different methods – contact measurement (DS18B20) and non-contact infrared thermography (unmanned and manual) – at each measurement point and at each recording moment (9:00, 12:00, 15:00 and 18:00), which is schematically summarized in Fig. 4. In cases where the sensor readings and thermography data coincided within the total instrumental error (±0.5°C for DS18B20 sensors; ±2°C or ±2% of the reading for thermal imagers, according to the manufacturer's specifications), the sensor value was taken as the main data array presented in Section 3, and the thermography data served as an independent cross-check. It is this double validation procedure that distinguishes the present measurement campaign from the field studies of VRF discussed in Section 1.2, which used only one measurement method.

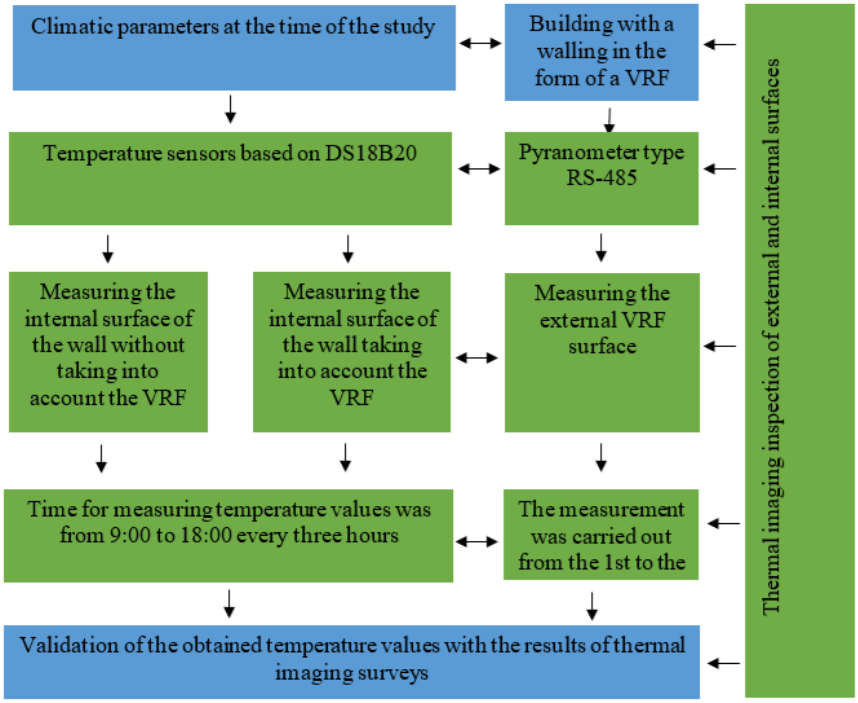


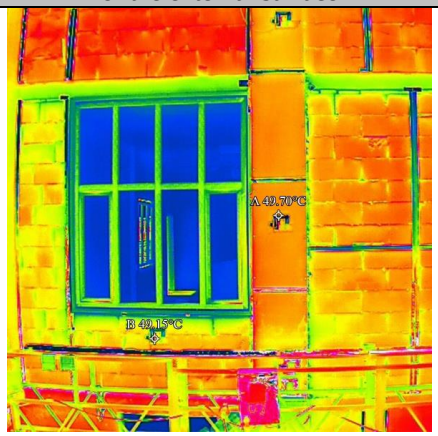
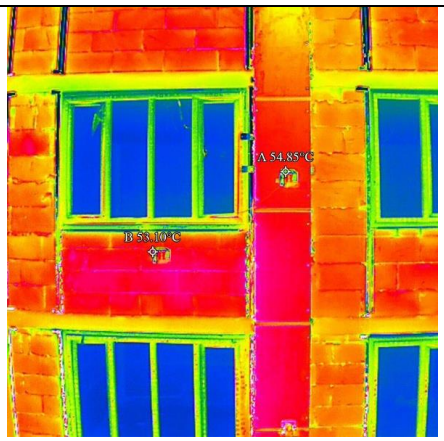
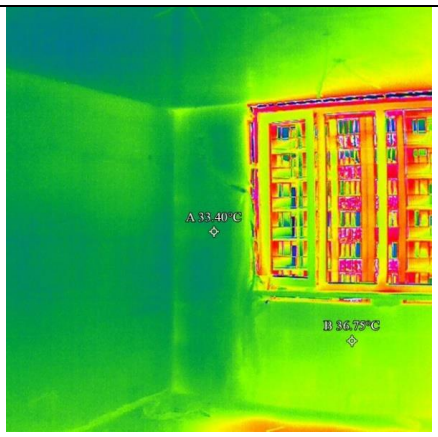
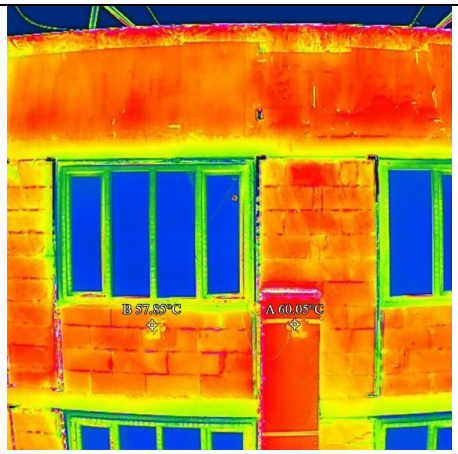
Fig. 4. Methodology of experimental research with parallel recording of temperature values on the surfaces of the walling.

3. RESULTS AND DISCUSSION

3.1. Validated Thermal Imaging of External and Internal Surfaces

As noted above, the in-kind study of the VRF effectiveness in a hot climate was conducted with parallel validation of the measured values in accordance with Fig. 4. Table 2 presents thermograms obtained during the hour of peak solar irradiation on the vertical surface of the eastern façade (12:00), and Table 3 presents a summary analysis of thermograms taken at 9:00, 15:00, and 18:00. This analysis yields temperature values for the external and internal surfaces of the walling, allowing: (i) to compare the temperature difference between areas with the installed VRF model and areas of the wet façade, and (ii) to conduct additional validation against the values obtained from contact temperature sensors.

Table 2. Thermograms of the external and internal surfaces of the walling at 12:00.

Floor	Thermograms of the external surface	Thermograms of the internal surface
I	 A=49.70°C/B= 49.15°C	 A=33.55°C/B=34.85°C
V	 A=54.85°C/B=53.10°C	 A=35.40°C/B=36.75°C
IX	 A=60.05°C/B=57.85°C	 A=37.60°C/B=39.05°C

**Index "A" indicates temperature values at a point located within the boundaries of a ventilated rainscreen façade (VRF), index "B" indicates a wet façade, for both the external and internal surfaces.*

Table 3. Generalized thermographic analysis of the external and internal surfaces of the walling.

Floor	Walling Surface Type	Thermogram Recording Time			
		9:00	12:00	15:00	18:00
I	External	A=46.15°C/ B=46.05°C	A=49.70°C/ B= 49.15°C	A=47.10°C/ B=46.70°C	A=40.05°C/ B=39.00°C
	Internal	A=32.05°C/ B=32.10°C	A=33.55°C/ B= 34.85°C	A=34.85°C/ B=36.40°C	A=35.20°C/ B=36.35°C
V	External	A=54.95°C/ B=54.45°C	A=54.85°C/ B=53.10°C	A=52.65°C/ B=51.05°C	A=44.40°C/ B=42.80°C
	Internal	A=33.50°C/ B= 34.10°C	A=35.40°C/ B=36.75°C	A=37.10°C/ B=38.50°C	A=36.95°C/ B=38.30°C
IX	External	A=58.15°C/ B=57.45°C	A=60.05°C/ B=57.85°C	A=58.55°C/ B=56.45°C	A=51.15°C/ B=49.05°C
	Internal	A=35.55°C/ B= 36.60°C	A=37.60°C/ B=39.05°C	A=38.85°C/ B=39.45°C	A=38.80°C/ B=39.25°C

**Index "A" indicates temperature values at a point located within the boundaries of a ventilated rainscreen façade (VRF), index "B" indicates a wet façade, for both the external and internal surfaces.*

Furthermore, in Fig. 5 and 6, to maintain the principle of reliability, the temperature values on the ventilated and wet surfaces of the walling, obtained using a universal sensor system, were additionally measured at various times during daylight hours and on different floors of the building.

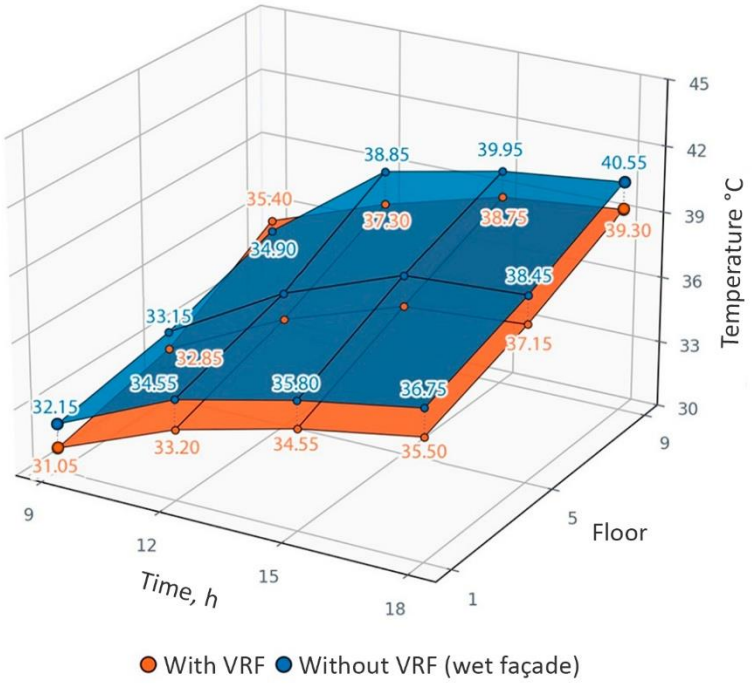


Fig. 5. Temperature of the internal surface of the walling with and without VRF.

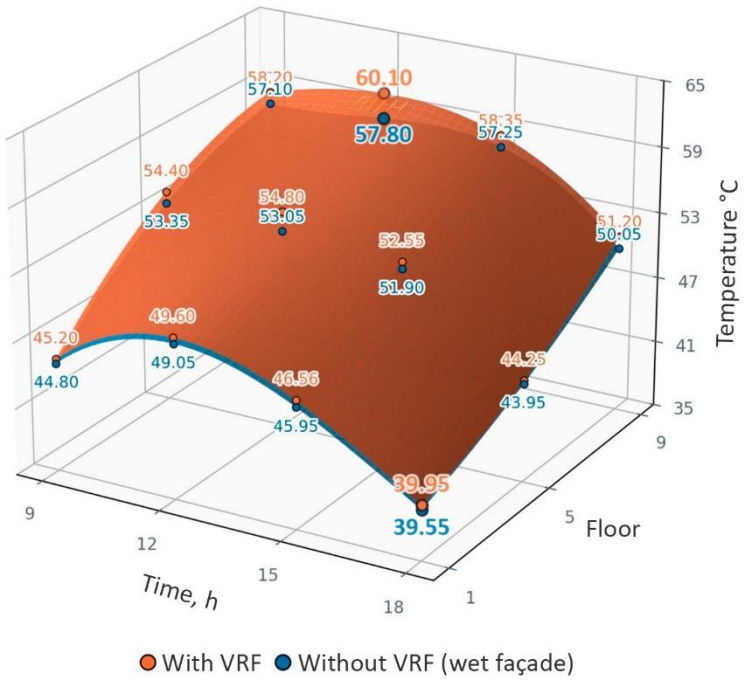


Fig. 6. Temperature of the external surface of the walling with and without VRF.

3.2. Daily Comparison of Internal Surface Temperatures: VRF and Wet Façade

Across all three monitored floors and all four recording times, the internal surface temperature of the VRF section, confirmed by the sensors, was lower than or statistically equal to the temperature of the wet façade section in 11 of the 12 measured floor-time combinations (Table 3, Figure 5). The instantaneous decrease in internal surface temperature,

$\Delta T_int.\ surf = T_int.\ surf,\ wet - T_int.\ surf,\ VRF,$

varyed from a minimum of 0.05°C (1st floor, 9:00, i.e., before significant solar heat load accumulation) to a maximum of 1.55°C (1st floor, 15:00). On average, across all 12 floor-time combinations, $\Delta T_int.surf = 1.03$°C; when limiting the sample to the two hottest moments of the day (12:00 and 15:00), the average decrease increases to $\Delta T_ext.surf \approx 1.28$ °C. The daily dynamics are indicative: the difference is minimal in the early morning (9:00), when the wall has not yet accumulated a significant solar heat load and both types of façade are close to thermal equilibrium with the internal environment, then increases during the day as the solar heat flux through the wet façade accumulates, and by 18:00 it narrows again as the solar influx decreases. This pattern holds true for all floors, although the absolute values of the internal surface temperatures increase with floor height (from approximately 32-35°C on the 1st floor to 36-39°C on the 9th floor at the same hour), reflecting the combined effect of greater unshaded solar exposure and greater sky irradiance on the upper floors, consistent with the vertical lapse rate of solar irradiation shown in Figure 3b.

3.3. The Paradox of the External-Internal Surface Relationship: Convective "Decoupling" in the Ventilated Interlayer

A noticeable and, at first glance, counterintuitive feature of the obtained data is that the relationship observed for the internal surface is inversely related to the external surface. In 10 of the 12 floor-time combinations, the temperature of the external cladding of the VRF (index A) exceeded the temperature of the wet façade (index B) – by an average of 1.22°C and up to 2.20°C (9th floor, 12:00 and 15:00). The external surface of the VRF reached a peak temperature of 60.05-60.10°C on the 9th floor at midday (Table 3, Figure 6). This is physically expected: the dark, low-heat-capacity ceramic granite cladding in the VRF, being thermally insulated from the load-bearing wall by an air gap, heats up

freely under direct solar irradiation to a greater extent than the directly plastered wet façade, which maintains continuous conductive contact with the more thermally capacious wall behind it.

The key result of this study is that a higher external surface temperature does not lead to a higher internal surface temperature, in fact, the opposite is true. This is explained by the ventilated nature of the air gap: since the air gap is open at the top and bottom, gravitational (and, secondarily, wind) convection continuously removes solar-heated air adjacent to the cladding before it has a chance to transfer significant heat by conduction and convection to the insulation and the load-bearing wall behind it. Essentially, the conductive heat path "seen" by the room-facing wall is "decoupled" from the peak equivalent temperature of the solar-irradiated cladding and is instead determined by the buffered temperature of the ventilating airflow, which is significantly lower than the temperature of the cladding surface itself. This mechanism is consistent with the behavior of the airflow in the interlayer under gravity convection and wind, described analytically and experimentally in the previous VRF literature [6-10, 12, 17], and is demonstrated directly for the first time, at a full-scale building scale and at floor-by-floor resolution, for the hot continental climate of Southern Kazakhstan, climatic conditions not previously represented in this literature (Section 1.2). From a practical perspective, this means that the external cladding temperature alone is a weak and potentially misleading indicator of the thermal benefit of VRF for the indoor environment, whereas the internal surface temperature, as directly measured in this study, represents a physically based index for assessing the cooling load implications.

3.4. Energy Efficiency of Cooling Systems Due to a Reduction in Internal Surface Temperature

To translate the measured internal surface temperature difference into an estimated gain in cooling energy delivery, the convective-radiant heat flux from the internal wall surface to the indoor air was estimated using the standard steady-state relationship

$$q = \alpha_{в} \cdot (T_{int.\,surf} - T_{room}),$$

where $\alpha_{в} = 8.7$ W/(m²·°C) is the internal surface heat transfer coefficient, traditionally adopted in regional building thermal engineering regulations for vertical external walls [30, 32, 33], and $T_{room} = 25$°C is adopted as the typical design summer indoor air temperature (air conditioning setpoint). Applying this relationship to the paired T_int.surf values from Table 3 for each floor and recording time allowed to calculate the percentage reduction in the conductive-convective component of the cooling load due to the use of the VRF, $(q_{wet} - q_{VRF})/q_{wet}$, for each of the 12 floor-time combinations. When limiting the assessment to typical daytime hours of the cooling load (12:00, 15:00, and 18:00, i.e. excluding the 9:00 value, at which the wall is close to thermal equilibrium and the cooling load is in any case minimal), the calculated reduction ranges from approximately 3% to 14% depending on the floor and hour, with an average of approximately 9.6%. When taking into account the entire day, including the 9:00 value, the average decreases to approximately 8.6%. Based on this, it can be expected that the conductive component of the cooling load for rooms behind the VRF is reduced by approximately 7-10% compared to an equivalent room behind a wet façade under the hot climate conditions and wall configuration considered here.

This estimate should be considered an approximate indicator, relating solely to the conductive component of the walling, and not as an indicator of the building's overall energy savings. It does not take into account internal heat gain, infiltration, glazing, room operating mode, and the efficiency of mechanical equipment, all of which also contribute to the total cooling energy delivery. However, it is derived directly and transparently from the field data presented in Sections 3.2-3.3, rather than from a separately calibrated building energy simulation model, which makes it methodologically different from most of the energy savings percentages reported in the literature discussed in Section 1.2 (e.g., [9, 17, 19]), and is offered here as a physically based, reproducible estimate suitable for a rough order-of-magnitude design assessment, pending the more detailed dynamic modeling discussed in Section 3.6.

3.5. Comparison with Previous Literature

The magnitude of the internal surface temperature reduction observed in the present study (up to 1.55°C, averaging around 1.0-1.3 °C during peak hours) is generally consistent with, although somewhat more modest, the 8-10°C interlayer temperature reduction and 30-40% cooling load reduction observed in comparisons of VRF and ETICS systems in Mediterranean climates with more favorable interlayer geometry and cladding configurations, as well as the 26% savings in summer recorded by Sanjuan et al. [9] for open-joint façades, and the 47-51% savings observed for naturally ventilated façades compared to non-ventilated façades under favorable wind conditions in other climate studies. This discrepancy is likely explained by the relatively narrow interlayer width (10 cm) used in the present VRF model (Table 1), the specific orientation (east) and absorptivity of the cladding of the tested structure, and the more pronounced continental character of the climate of Southern Kazakhstan (larger diurnal temperature difference, lower relative humidity, different wind regime) compared to the coastal and subcontinental Mediterranean sites prevailing in the reviewed literature [4, 5, 7-10, 17, 21-23]. Nevertheless, the obtained result confirms for the first time, in relation to these specific climatic conditions, the qualitative mechanism established in this literature, while simultaneously showing that quantitative gains should not be automatically transferred from indicators calibrated for the Mediterranean climate without in-kind local verification, which was the specific gap that the present study aimed to close (Sections 1.5-1.6).

3.6. Limitations and Directions for Further Research

This article is part of a larger, ongoing research program by the authors' team devoted to the performance of ventilated façades in the climatic conditions of Southern Kazakhstan [35-37], and the results presented here should be considered in this context. In particular, the present study characterizes the surface temperature field of the VRF and wet façade and its influence on the cooling load, but does not reveal the internal thermo-aerodynamic structure of the ventilated interlayer itself: how the air temperature and velocity in the interlayer, as well as the heat transfer coefficient, vary with height along the nine-story façade and during the day, and how solar-induced heating of the air in the interlayer, in turn, changes the velocity of the gravity-convection flow in hot climates, remain open questions that the accompanying aerodynamic models reported in the literature [43] address only partially. These effects of thermal-aerodynamic interaction, temperature and velocity profiles in the interlayer with vertical resolution, their diurnal dynamics, and sensitivity to the interlayer width and wind exposure, will be the subject of further in-situ experimental and CFD studies by the authors. This paper is deliberately limited in scope to demonstrate, based on twice-validated in-situ measurements, the practical thermal performance of the VRF compared to a wet façade in the hot climate of Southern Kazakhstan; the underlying flow mechanics in the interlayer is left for this future work. Additional limitations include: conducting the measurement campaign for a single orientation (east) and over a single day, which, although representative of a hot summer day according to the regional climatology data of SP RK 2.04-01-2017, does not reflect interdiurnal and interseasonal variability; as well as the approximate nature of the cooling efficiency assessment in Section 3.4, which would benefit from comparison with the energy meter readings of the air conditioning system in the building in use.

4. CONCLUSIONS

1. A field-based, double-validated measurement campaign (contact sensors, unmanned and handheld thermal imaging) on a nine-story residential building in Southern Kazakhstan demonstrated that a ventilated rainscreen façade (VRF) provides lower internal (room-facing) surface temperatures compared to an adjacent traditional wet (plastered) façade on virtually all floors examined and at all times, with a reduction of up to 1.55°C and an average reduction of approximately 1.0-1.3°C during the hottest hours of the day.
2. This advantage on the internal surface is achieved despite the fact that the VRF external cladding heats up to 2.2°C higher than the wet façade during peak insolation hours (up to 60.1°C on the ninth floor at midday). This apparent paradox is explained by convective "uncoupling" within the ventilated air gap, which removes solar-heated air before it can transfer heat to the load-bearing wall.

Therefore, the external surface temperature alone is not a reliable indicator of the VRF's benefit to the internal thermal environment.

3. Based on the measured internal surface temperature difference and the standard internal surface heat transfer coefficient, it was shown that the conductive component of the cooling load for rooms behind the VRF is approximately 7-10% lower than for an equivalent room behind a wet façade, under the hot climate conditions studied. This represents a physically based performance indicator, derived from field data, and not the result of simulation alone.

4. The obtained results, related to the relatively little-studied hot arid/continental climate of Central Asia, expand the evidence base formed primarily based on Mediterranean and Western European studies and provide Southern Kazakhstan and comparable regions of Central Asia with field-confirmed, rather than transferable, recommendations for the design of VRFs for reconstruction and new construction.

5. As part of a broader research program, this work is limited in scope to a comparison of surface temperatures and cooling efficiency; the internal thermal and aerodynamic behavior of the ventilated interlayer, including the dynamics of temperature and air velocity in the interlayer with height and time resolution and their interrelationships under solar loading in a hot climate, will be investigated in subsequent studies by the authors.

5. ACKNOWLEDGEMENTS

This research is funded by the Science Committee of the Ministry of Science and Higher Education of the Republic of Kazakhstan (Grant No. AP23486892)

REFERENCES

1. International Energy Agency (IEA). Energy Efficiency 2025 – Buildings. Paris: IEA, 2025. URL: https://www.iea.org/reports/energy-efficiency-2025/buildings
2. International Energy Agency (IEA). World Energy Outlook 2024. Paris: IEA, 2024. URL: https://www.iea.org/reports/world-energy-outlook-2024
3. International Energy Agency (IEA). Staying Cool without Overheating the Energy System. Paris: IEA, 2025. URL: https://www.iea.org/commentaries/staying-cool-without-overheating-the-energy-system
4. Ibañez-Puy M., Vidaurre-Arbizu M., Sacristán-Fernández J.A., Martín-Gómez C. Opaque ventilated façades: Thermal and energy performance review. Renewable and Sustainable Energy Reviews. 2017. 79. P. 180 – 191. DOI: https://doi.org/10.1016/j.rser.2017.05.059
5. Pizzatto S., Pizzatto F., Raupp-Pereira F., Arcaro S., Angioletto E., Montedo O. Ventilated facade system: A review. Boletín de la Sociedad Española de Cerámica y Vidrio. 2025. 64. 100443. DOI: https://doi.org/10.1016/j.bsecv.2025.100443
6. Balocco C. A simple model to study ventilated facades energy performance. Energy and Buildings. 2002. 34. P. 469 – 475. DOI: https://doi.org/10.1016/S0378-7788(01)00130-X
7. Ciampi M., Leccese F., Tuoni G. Ventilated facades energy performance in summer cooling of buildings. Solar Energy. 2003. 75. P. 491 – 502. DOI: https://doi.org/10.1016/j.solener.2003.09.010
8. Gratia E., De Herde A. Natural cooling strategies efficiency in an office building with a double-skin façade. Energy and Buildings. 2004. 36. P. 1139 – 1152. DOI: https://doi.org/10.1016/j.enbuild.2004.05.004
9. Sanjuan C., Suárez M.J., González M., Pistono J., Blanco E. Energy performance of an open-joint ventilated façade compared with a conventional sealed cavity façade. Solar Energy. 2011. 85. P. 1851 – 1863. DOI: https://doi.org/10.1016/j.solener.2011.04.028
10. Marinosci C., Strachan P.A., Semprini G., Morini G.L. Empirical validation and modelling of a naturally ventilated rainscreen façade building. Energy and Buildings. 2011. 43. P. 853 – 863. DOI: https://doi.org/10.1016/j.enbuild.2010.12.005

11. Stazi F., Tomassoni F., Vegliò A., Di Perna C. Experimental evaluation of ventilated walls with an external clay cladding. Renewable Energy. 2011. 36. P. 3373 – 3385. DOI: https://doi.org/10.1016/j.renene.2011.05.016
12. Labat M., Woloszyn M., Garnier G., Rusaouen G., Roux J.J. Impact of direct solar irradiance on heat transfer behind an open-jointed ventilated cladding: experimental and numerical investigations. Solar Energy. 2012. 86. P. 2549 – 2560. DOI: https://doi.org/10.1016/j.solener.2012.05.030
13. Gagliano A., Patania F., Nocera F., Ferlito A., Galesi A. Thermal performance of ventilated roofs during summer period. Energy and Buildings. 2012. 49. P. 611 – 618. DOI: https://doi.org/10.1016/j.enbuild.2012.03.007
14. Yu J., Yang J., Xiong C. Study of dynamic thermal performance of hollow block ventilated wall. Renewable Energy. 2015. 84. P. 145 – 151. DOI: https://doi.org/10.1016/j.renene.2015.07.020
15. Tong S., Li H. An efficient model development and experimental study for the heat transfer in naturally ventilated inclined roofs. Building and Environment. 2014. 81. P. 296 – 308. DOI: https://doi.org/10.1016/j.buildenv.2014.07.009
16. Zhao X., Dugue A., Bonnamy P., Javier Miguel F., Martinez A., Theodosiou T., Liu J.-S., Brown N. Numerical investigation of the energy performance of an Opaque Ventilated Façade system employing a smart modular heat recovery unit and a latent heat thermal energy system. Applied Energy. 2017. 205. P. 130 – 152. DOI: https://doi.org/10.1016/j.apenergy.2017.07.042
17. Gagliano A., Aneli S. Analysis of the energy performance of an opaque ventilated façade under winter and summer weather conditions. Solar Energy. 2020. 205. P. 531 – 544. DOI: https://doi.org/10.1016/j.solener.2020.05.078
18. Karanafti A., Theodosiou T., Tsikaloudaki K. Assessment of buildings' dynamic thermal insulation technologies – A review. Applied Energy. 2022. 326. 119920. DOI: https://doi.org/10.1016/j.apenergy.2022.119985
19. Lin Z., Song Y., Chu Y. An experimental study of the summer and winter thermal performance of an opaque ventilated facade in cold zone of China. Building and Environment. 2022. 218. 109108. DOI: https://doi.org/10.1016/j.buildenv.2022.109108
20. Karanafti A., Theodosiou T. Summer thermal performance analysis of an Opaque ventilated Façade operating under the dynamic insulation principle. Energy and Buildings. 2024. 312. 114193. DOI: https://doi.org/10.1016/j.enbuild.2024.114193
21. Domínguez-Torres C.A., Suárez R., León-Rodríguez Á.L., Domínguez-Delgado A. Parametric energy optimization of a ventilated facade with windows in Mediterranean climates. Renewable Energy. 2024. 227. 120398. DOI: https://doi.org/10.1016/j.renene.2024.120398
22. Roig O., Summa S., Pardal C., Isalgue A., Di Perna C., Stazi F. Opaque ventilated façades: Energy performance for different main walls and claddings. Energy and Buildings. 2024. 314. 114280. DOI: https://doi.org/10.1016/j.enbuild.2024.114280
23. De Masi R.F., Ruggiero S., Vanoli G.P. Hygro-thermal performance of an opaque ventilated façade with recycled materials during winter time. Energy and Buildings. 2024. 315. 114294. DOI: https://doi.org/10.1016/j.enbuild.2021.110994
24. Pankratov E.L. A Model of Distribution of Temperature in A Ventilated Facades. Advanced Engineering Technology and Application. 2025. 14 (1). P. 1 – 6. DOI: https://doi.org/10.18576/aeta/140101
25. Di Nunzio G., Al-Mansouri O., Muciaccia G., Gabs A. In-plane behaviour of lightweight façade systems installed in masonry and concrete under simulated seismic loading. Journal of Building Engineering. 2023. 63. 105442. DOI: https://doi.org/10.1016/j.jobe.2022.105442
26. Tabatabaei S., Fayaz R. The effect of facade materials and coatings on urban heat island mitigation and outdoor thermal comfort in hot semi-arid climate. Building and Environment. 2023. 243. 110701. DOI: https://doi.org/10.1016/j.buildenv.2023.110701

27. Hong C., Wang Y., Gu Z., Yu C.W. Cool facades to mitigate urban heat island effects. Indoor and Built Environment. 2022. 31. P. 2409 – 2427. DOI: https://doi.org/10.1177/1420326X221115369
28. Maciel A.C.F., Carvalho M.T. Methodology used to investigate the energy savings of opaque ventilated façades in residential buildings in Brazil. MethodsX. 2021. 8. 101227. DOI: https://doi.org/10.1016/j.mex.2021.101227
29. Wang Y., Chen Y., Zhou J. Dynamic modeling of the ventilated double skin façade in hot summer and cold winter zone in China. Building and Environment. 2016. 106. P. 365 – 377. DOI: https://doi.org/10.1016/j.buildenv.2016.07.012
30. International Organization for Standardization. ISO 6946:2017. Building Components and Building Elements – Thermal Resistance and Thermal Transmittance – Calculation Methods. Geneva: ISO, 2017.
31. Al-Sanea S.A., Zedan M.F. Improving thermal performance of building walls by optimizing insulation layer distribution and thickness for same thermal mass. Applied Energy. 2011. 88. P. 3113–3124. DOI: https://doi.org/10.1016/j.apenergy.2011.02.036
32. Zhangabay N., Tursunkululy T., Ibraimova U., Abdikerova U. Energy-efficient adaptive dynamic building facades: A review of their energy efficiency and operating loads. Applied Sciences. 2024. 14. 10979. DOI: https://doi.org/10.3390/app142310979
33. Rahiminejad M., Khovalyg D. Experimental study of the hydrodynamic and thermal performances of ventilated wall structures. Building and Environment. 2023. 233. 110114. DOI: https://doi.org/10.1016/j.buildenv.2023.110114
34. Zhangabay N., Zhangabay A., Utelbayeva A., Tursunkululy T., Zakaria R., Bakhbergen S. Full-scale experimental investigation of the influence of solar radiation on the thermal behavior of ventilated façade envelope systems under hot climate conditions. Buildings. 2026. 16. 122. DOI: https://doi.org/10.3390/buildings16010122
35. Duissenbekov B., Tokmuratov A., Orazbayev Zh., Yerimbetov B., Aldiyarov Zh. Finite-difference equations of quasistatic motion of the shallow concrete shells in nonlinear setting. Curved and Layered Structures. 2020. 7 (1). P. 48 – 55. DOI: https://doi.org/10.1515/cls-2020-0005
36. Borodin K., Zhangabay N. Mechanical characteristics, as well as physical-and-chemical properties of the slag-filled concretes, and investigation of the predictive power of the metaheuristic approach. Curved and Layered Structures. 2019. 6 (1). P. 236 – 244. DOI: https://doi.org/10.1515/cls-2019-0020
37. Zhangabay N., Ibraimova U., Suleimenov U., Moldagaliyev A., Buganova S., Jumabayev A., Kolesnikov A., Tursunkululy T., Zhiyenkulkyzy D., Khalelova A., et al. Factors affecting extended avalanche destructions on long-distance gas pipe lines: Review. Case Studies in Construction Materials. 2023. 19. e02376. DOI: https://doi.org/10.1016/j.cscm.2023.e02376
38. Shcherban' E.M., Beskopylny A.N., Stel'makh S.A., Mailyan L.R., Shilov A.A., Nguyen Q.H., Yamin S., Chernil'nik A.A., Elshaeva D.M. Study of thermophysical characteristics of variatropic concretes. Construction Materials and Products. 2024. 7 (4). P. 2. DOI: https://doi.org/10.58224/2618-7183-2024-7-4-2
39. Naumov A.E., Suvorova M.O., Bakaeva N.V., Danilina N.V. Building life-cycle management by carbon homeostasis potential. Construction Materials and Products. 2024. 7 (4). P. 8. DOI: https://doi.org/10.58224/2618-7183-2024-7-4-8
40. Petropavlovskaya V.B., Petropavlovskii K.S., Novichenkova T.B., Klyuev S.V., Vasilev Yu.E., Ignatyev A.A. Fine-grained cement concrete with compressed structure, modified with basalt technogenic highly dispersed powder. Construction Materials and Products. 2025. 8 (4). P. 17 – 36. DOI: https://doi.org/10.58224/2618-7183-2025-8-4-2
41. Fedosov S.V., Aleksandrova O.V., Bakanov M.O. Heat and mass transfer in concrete mixtures during transportation along the route «Manufacturer of liquid-phase solution – consumer of solid-phase concrete». Construction Materials and Products. 2025. 8 (6). P. 6. DOI: https://doi.org/10.58224/2618-7183-2025-8-6-6

42. Sargsyan S.V., Agafonova V.V. Influence of heat resistance of the enclosing structures of a heated room on the choice of the type and location of the heating device. Construction Materials and Products. 2026. 9 (1). P. 5. DOI: https://doi.org/10.58224/2618-7183-2026-9-1-5
43. Zhangabay N., Zhangabay A., Utelbayeva A., Bonopera M., Akmalaiuly K., Tursunkululy T. Thermo-aerodynamic response of a multilayer ventilated façade under high solar radiation: A full-scale, full-height experimental analysis of a 0.6-m-wide instrumented test channel on a nine-storey residential building. Results in Engineering. 2026, P.112785. DOI: https://doi.org/10.1016/j.rineng.2026.112785

INFORMATION ABOUT THE AUTHORS

Zhangabay N.Zh., e-mail: Nurlan.Zhanabay777@mail.ru, ORCID ID: https://orcid.org/0000-0002-8153-1449, SCOPUS: https://www.scopus.com/authid/detail.uri?authorId=57211557292, Kazakhstan, M. Auezov South Kazakhstan University, Department of Scientific Research Laboratory of Mechanical Engineering Problems, Candidate of Technical Sciences (PhD), Associate Professor

Suleimenov U.S., e-mail: ulanbator@inbox.ru, ORCID ID: https://orcid.org/0000-0001-7798-1044, SCOPUS: https://www.scopus.com/authid/detail.uri?authorId=56698407200&origin=resultslist, Kazakhstan, M. Auezov South Kazakhstan University, Department of Architecture and Urban Planning, Doctor of Technical Sciences (Advanced Doctor), Professor

Utelbayeva A.B., e-mail: mako_01-777@mail.ru, ORCID ID: https://orcid.org/0000-0002-4771-9835, SCOPUS: https://www.scopus.com/authid/detail.uri?authorId=57151414400, Kazakhstan, M. Auezov South Kazakhstan University, Department of Chemistry, Doctor in Chemistry (Advanced Doctor), Associate Professor

Aidarova A.B., e-mail: ab_moon@mail.ru, ORCID ID: https://orcid.org/0000-0002-5503-641X, SCOPUS: https://www.scopus.com/authid/detail.uri?authorId=56613448000, Kazakhstan, M. Auezov South Kazakhstan University, Department of Economics, Candidate in Economic Sciences (PhD), Professor

Kolesnikov A.S., e-mail: kas164@yandex.kz, ORCID ID: https://orcid.org/0000-0002-8060-6234, SCOPUS: https://www.scopus.com/authid/detail.uri?authorId=57189499212, Kazakhstan, M. Auezov South Kazakhstan University, Department of Life Safety and Environmental Protection, Candidate of Technical Sciences (PhD), Professor

Tursunkulov I.B., e-mail: ikhtiyar.tursunkulov@mail.ru, ORCID ID: https://orcid.org/0009-0009-0901-1551, Kazakhstan, M. Auezov South Kazakhstan University, Department of Architecture and Urban Planning

Tursunkululy T., e-mail: timurtursunkululy@gmail.com, ORCID ID: https://orcid.org/0000-0001-6215-7677, SCOPUS: https://www.scopus.com/authid/detail.uri?authorId=57687675500, Kazakhstan, M. Auezov South Kazakhstan University, Department of Architecture and Urban Planning, Candidate of Engineering Sciences (Ph.D.)

Nazmi M.N., e-mail: nazmimat@upm.edu.my, ORCID ID: https://orcid.org/0000-0002-5916-5745, SCOPUS: https://www.scopus.com/authid/detail.uri?authorId=57189925855, Malaysia, Universiti Putra Malaysia, Head of Fakulty of Engineering, Candidate of Engineering Sciences (Ph.D.), Associate Professor